Assessment of the Possibility of Using Fractal Analysis to Describe the Surface of Aluminum Composites After Turning

Paweł Karolczak[1], Maciej Kowalski[1], Katarzyna Raszka[1]

[1] Wroclaw University of Science and Technology, Faculty of Mechanical Engineering, ul. Łukasiewicza 5, 50-371 Wrocław, Poland

* Corresponding author's e-mail: pawel.karolczak@pwr.edu.pl

ABSTRACT

The description of the characteristics of the surface using standardized roughness parameters can not fully predict its performance properties. One of the tools supporting the assessment of the surface layer of the treated surface may be fractal analysis. This applies both to surfaces with machining traces, which are created under conditions of high randomness and variability of process conditions, and to surfaces with directional traces and their distinct periodicity. The paper presents the results of surface roughness measurements of turned aluminium matrix composites reinforced with ceramic fibers. Carbide and diamond tools were used for turning the tested material. The trials were carried out under dry machining conditions and with minimal lubrication in the cutting zone. Surfaces were measured by the contact method, and surface roughness parameters were calculated by Gaussian filtration. Then, the values of the fractal dimension were calculated using the enclosing box method. On the basis of these calculations, the influence of machining conditions on the values of selected roughness parameters and the box fractal dimension was determined. It was found that the fractal dimension, i.e. the irregularity of the geometric structure of the surface after turning of composites, changes with the change of cutting parameters, the tool and the method of lubricating the cutting zone. Of these factors, the feed has the greatest influence. As it grows, the irregularity of the machined surface structure decreases. In addition, the correlation coefficients between the fractal dimension and the measured roughness parameters were determined. It was noticed that the fractal dimension, in the case of turning aluminum composites, best correlates with the roughness parameters *Sa* and *Ssk* and thus describes features similar to these parameters. Therefore, it was assumed that it is possible to use fractal analysis as a supplementary tool for the description of the surface condition of aluminum composites after turning in various machining conditions. On the other hand, the fractal dimension can be treated as an additional tool to describe the surface condition, especially its irregularity, which is not described by other standard roughness parameters.

Keywords: fractal analysis, surface roughness, composite materials, cutting zone lubrication, diamond.

INTRODUCTION

Because of their excellent mechanical and strength properties combined with their light specific weight, composite materials are used in many branches of industry. They are the main construction materials for air transport means [1]. Composites consist of a matrix and a reinforcement. The latter most often has the form of fibres and particles. The matrix is made of lightweight materials such as metals, polymers, and ceramics. The first industrially used composites were based on aluminium [2]. They are still popular and widely used. They are most often produced by stir-casting, and their reinforcement is made of, eg, silicon carbide, boron carbide, or fly ash [3]. Due to the peculiar properties of aircraft composite materials, the latter are classified as poorly machinable. Furthermore, due to the rigorous quality requirements of aviation, numerous difficulties arise during the machining of composites. Metallic composite materials are anisotropic and heterogeneous, and the presence of strongly abrasive reinforcement results in rapid wear of the cutting tool. The hardness and abrasiveness of the reinforcement are not the only cause of heavy tool wear.

Since the tool is in alternating contact with the soft matrix and the reinforcement material, it is subject to variable loads and, thus, fatigue wear. It may also cause damage to the workpiece [4, 5]. Therefore, the quality control of composite products is very important. It should guarantee that any surface defects are detected and make it possible to forecast the functional characteristics of the surface with the most precision. Conventional methods for describing geometrical surface and roughness structures do not guarantee this. Moreover, surface roughness is classified as a signal, at least partially nonstationary and variable, which can make the analysis difficult. Therefore, novel methods of describing the surface are sought. A promising novel method is fractal analysis. Fractals are objects characterized by self-similarity, which applies to both the whole object and its parts. The concept of fractals was introduced by the mathematician Benoit Mandelbrot, who used fractals to describe the coastline of Great Britain [6]. Owing to their peculiar characteristics, fractals are used today for analytical purposes in many fields of science and life. Many scientists have used fractals to analyse experimental results. Such an analysis mainly consists of calculating the specific dimension of the analysed object or signal. This dimension is called a fractal dimension, and there are many ways to determine it. For the analysis of images and graphics, and so also surface roughness, the box method is most often used. This method is considered the most reliable and yields the most reliable results [7].

An example can be the investigations presented in [8], where the fractal dimension was calculated using the box method and the influence of the surface quality of the workpiece and the cutting parameters on the fractal dimension was assessed. It was found that the fractal dimension is mainly affected by the cutting speed and the feed rate. Fractal dimension can help measure surface roughness [9, 10] and predict surface roughness [11]. Fractal analysis is also used as a criterion to investigate thin-layer surfaces [12] and soft layers [13]. Using the fractal dimension, one can evaluate not only the quality of the product, but also the degree of wear of the mating surface [14], which allows one to assess the likely lifetime of objects more quickly and efficiently. Furthermore, the fractal dimension may be one of the parameters of the fracture surface topography assessment due to the fatigue load mode [15, 16]. Describing the condition of a surface fractal analysis is often combined with other image decomposition methods, such as wavelet analysis [17]. Research on applying both methods to the evaluation of the measured surface quality and the characterization of the machined surface can be found in [18, 19]. In manufacturing techniques, fractal analysis is used to assess other associated phenomena and effects, such as acoustic emission or cutting forces [20], which occur not only in cutting, but also in electrical discharge machining [21] and abrasive machining [22, 23]. Attempts have also been made to use fractal analysis to assess the effects of the machining of composite materials [24, 25]. Unfortunately, as composites have a heterogeneous structure and incorporate two or more materials that differ radically in their properties, an analysis of the machining process in their case is not easy [26]. Furthermore, the number of industrially used and scientifically studied composites continues to increase. Their hybrid varieties, consisting of many components, gain in importance. Consequently, more research is needed to effectively use fractal analysis to describe the condition of the machined surface of composites, both for a specific kind of composite and for a whole group of materials. The tests presented in this paper aimed to expand the knowledge about the quality of the surface of aluminum composites after turning with carbide and diamond tool inserts under dry and MQL machining conditions. The experimental results reported here complement those presented in [27].

TESTING CONDITIONS

An aluminium composite material was subjected to tests. Complex casting aluminium alloy AlSi9Mg, constituted the matrix and Saffil ceramic fibres were the reinforcement. The matrix is characterized by lower hot brittleness and good resistance to corrosion and action of seawater. The alloy is readily machinable, weldable and well castable. The composite's strength is determined by its reinforcement. The Saffil fibres constituting the reinforcement are a popular material used for reinforcing aluminium composites. The fibres consist of 96–97% Al_2O_3 and 3–4% SiO_2. They are classified as high-strength materials as they are characterized by high-temperature resistance (are durable up to the temperature of 1600 °C), high tensile strength (1.8 GPa) and a high E-modulus (300 GPa). Owing to the properties of the
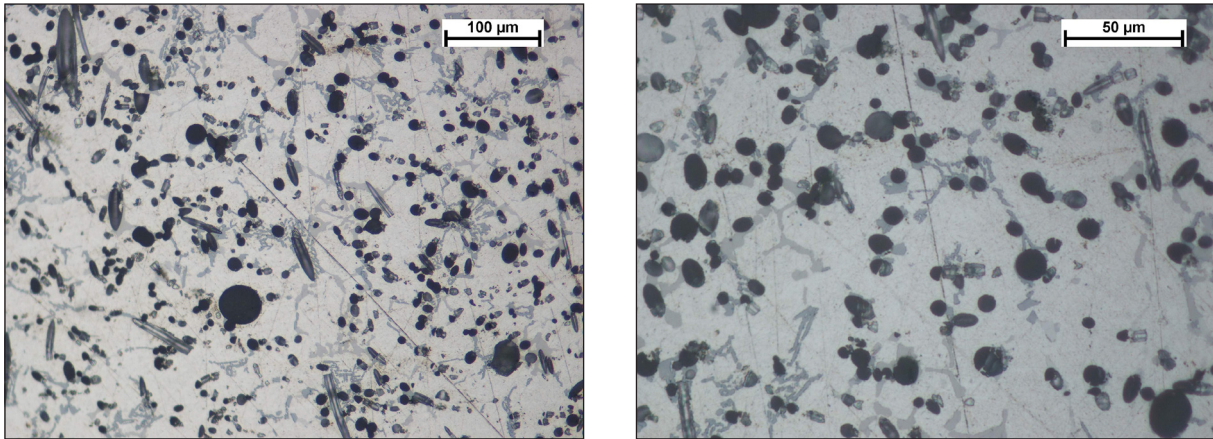
Fig. 1. Structure of tested material; left – 200x magnification, right – 500x magnification

reinforcing fibres, the composite, compared with the matrix, is characterized by increased hardness (by 50%) and tensile strength (by 60%). Also, its offset yield strength increases (by 40%). The composite's smaller elongation has a positive effect on its machinability, whereby the intensity of edge buildup during the machining of the composite is reduced. The tested material was produced using squeeze casting. The sintered fibre block was infiltrated with the matrix liquid metal. A microscopic photograph of the structure of the tested composite is shown in Figure 1.

Composite material turning tests were carried out on a CNC TUR 560 MN lathe. The lathe was equipped with a Siemens SINUMERIK 810 Manual Turn control and an AC system. The tests were carried out for a wide range of cutting parameters characteristic of both roughing and finishing, i.e. v_c = 150, 450 and 900 m/min and f = 0.08, 0.13 and 0.27 mm/rev. The depth of cut amounted to a_p = 0.5 mm. The turning tests were conducted in dry cutting conditions and at minimum quantity lubrication (MQL) with oil mist. A MiniBooster MB II HDC feeder made by Accu-Lube was used to produce oil mist. The feeder is suitable for both internal and external lubrication. It is equipped with two cutting fluid tanks from which the fluid is pumped via hoses to nozzles. The amount of the fed fluid is adjusted through a valve and a pump speed governor. Oil mist was fed via two hoses to the tool flank and face. Oil LB 5000 (based on fatty alcohol), recommended

for aluminium machining, was used. The oil is non-toxic and environmentally safe. The oil mist flow rate amounted to 125 ml/h.

Two kinds of cutting tools were used in the tests. Since an aluminium alloy constituted the tested material's matrix, tools (tool materials) recommended for the machining of this group of materials were used in the tests. One of the tools was a TCGX16T304–Al H10 insert made of uncoated sintered carbide. The insert's main advantage is its small cutting edge corner radius r_n = 0.005 mm. Sharp cutting edge geometry is recommended for the machining of soft aluminium alloys. The other tool was a TCMW 16T3 04F–CD10 insert made of polycrystalline diamond. The latter guarantees longer tool life in machining this type of composites [27]. Each of the inserts was fixed in an STGCR 2020K–16 frame. Surface roughness measurements were performed using a Mitutoyo SV series 3200 profilographometer. A diamond stylus with a cone corner radius of 2 µm and an angle of 60° was used for the measurements. The stylus tip pitch amounted to 800 micrometres. The FORMTRACEPACK measurement software was used. The profilographometer was equipped with a 3D measuring table with a resolution of 0.05 µm and the McCube Ultimate software for 3D analysis. After the machining tests, each of the surface was measured three times. A 1 mm × 1 mm area was measured. The step of measurement from the x-axis amounted to 5 µm. Also, the 3D measuring table would be shifted by 5 µm. As a result, 40000

Table 1. Properties of LB 5000 oil used to generate oil mist [28]

LB 5000 oil	Density [kg/m³]	Solidification Temperature	Flash point	Stickiness in 40°c	Solubility in water
	850	5 °C	190 °C	18	insoluble

points would be collected in each measurement. After the measurements, the McCube Ultimate software was used to analyse and calculate surface roughness. Using the software, measurement was levelled, shape errors were removed and surface waviness was separated from surface roughness by the Gaussian filter. Then, by the relevant ISO standard, the 3D roughness parameters were calculated. Finally, the box fractal dimension was calculated for the measured surfaces. The dimension commonly used in fractal analysis is the box dimension. It is characterized by the greatest universality. Measurements can be performed for both planes and three-dimensional spaces. The idea of this method is simple and consists in superimposing a regular grid with constant-size components on the measured structure. Depending on the investigative dimension (2D/3D), the components assume the form of squares or cubes – "boxes" of constant size ε. Then it is counted in how many of the components the measured structure $N(\varepsilon)$ occurs. This process is repeated for a smaller size ε and $\ln(N(\varepsilon))/\ln(\varepsilon)$ graph is plotted.

The work uses the method of calculating box dimension called enclosing boxes. The method consists of enclosing each section of a profile by a box of width ε (in points) and calculating the area $A\varepsilon$ of all the boxes enclosing the whole profile. This procedure is iterated with boxes of different widths to build a graph $\ln(A\varepsilon)/\ln(\varepsilon)$. This method can be extended to build a volume graph $\ln(V\varepsilon)/\ln(\varepsilon)$ for surfaces.

The fractal dimension is calculated from the slope of a regression line The accuracy of the calculations was set to be exact. This setting determines the number of iterations and therefore the calculation time. The value of ε varied in the range of 25–235 µm. This is the largest range possible to set in the McCube software. The step with which the ε value was changed in subsequent iterations was 10 µm for boxes with a side ε of 25–135 µm and 20 µm for boxes with a side ε 135–235 µm.

TEST RESULTS AND DISCUSSION

The profilographometer can measure 2D and 3D surface roughness profiles. Both 2D and 3D measurements were performed during the tests. Through 3D measurements, one can determine both parameters corresponding to the ones found in the standards for 2D measurements and parameters which can be calculated only for spatial roughness structures. However, it was decided that only spatial calculations will be presented in this paper. Four roughness height parameters: *Sa*, *Sz*, *Ssk* and *Sku*, were selected for further analyses. The first of the parameters is needed for a quantitative assessment, the second one for an assessment of the occurrence of single roughness valleys and

Table 2. Surface roughness parameters of composites after turning with tool made of sintered carbide H10

| Parameters					Fractal dimension *D*	*Sa* [µm]	*Sz* [µm]	*Ssk* [-]	*Sku* [-]
Cutting speed v_c [m/min]	150	Machining conditions	dry	Feed rate *f* [mm/rev]	0.08	2.61	0.87	15	-0.13	4.53
					0.13	2.53	1.64	18.5	0.16	3.28
					0.27	2.46	2.64	27	0.38	3.08
			MQL		0.08	2.58	0.8	11.01	0.2	4.62
					0.13	2.49	1.18	12.25	0.26	2.56
					0.27	2.42	1.56	8.32	0.79	2.89
	450		dry		0.08	2.56	0.9	17.05	0.67	5.86
					0.13	2.45	1.4	11.94	0.62	2.49
					0.27	2.28	2.45	13.85	1.22	3.39
			MQL		0.08	2.52	0.32	6.59	-0.76	6.7
					0.13	2.31	0.62	7.16	0.63	4.25
					0.27	2.3	1.41	10.9	0.84	3.14
	900		dry		0.08	2.64	1.34	17.9	0.32	3.89
					0.13	2.54	1.54	16.55	0.19	3.09
					0.27	2.31	2.78	19.8	1.01	3.35
			MQL		0.08	2.44	0.35	5.32	0.3	4.02
					0.13	2.3	0.55	7.11	1.05	3.95
					0.27	2.21	1.31	9.67	1.16	3.55

Table 3. Surface roughness parameters after turning with tool made of polycrystalline diamond CD10

Parameters					Fractal dimension *D*	*Sa* [µm]	*Sz* [µm]	*Ssk* [-]	*Sku* [-]
Cutting speed *v_c* [m/min]	150	Machining conditions	dry	Feed rate *f* [mm/rev]	0.08	2.72	0.54	4.31	0.09	1.76
					0.13	2.38	0.92	6.6	0.71	2.59
					0.27	2.24	2.63	13.05	1.08	2.8
			MQL		0.08	2.66	0.59	4.17	0.14	1.92
					0.13	2.37	0.99	7.27	0.54	2.49
					0.27	2.22	2.67	15.3	1.12	3.02
	450		dry		0.08	2.64	0.8	8.83	-0.22	2.73
					0.13	2.34	0.91	5.65	0.66	2.51
					0.27	2.25	2.62	13.65	1.04	2.91
			MQL		0.08	2.68	0.61	3.7	0.14	1.8
					0.13	2.42	1.12	10.41	0.13	2.45
					0.27	2.25	2.74	16.95	1.04	3.08
	900		dry		0.08	2.59	0.59	3.53	0.02	2.08
					0.13	2.39	0.94	7.67	0.67	2.72
					0.27	2.3	2.71	20.3	0.88	2.74
			MQL		0.08	2.65	0.65	5.17	-0.03	2.27
					0.13	2.34	0.98	7.4	0.5	2.39
					0.27	2.2	2.52	17.9	1.24	3.44

elevations while *Ssk* and *Sku* are needed for a surface quality assessment. The results of the measurements of the selected roughness parameters and the calculated box fractal dimension values are presented in Table 2 and 3. One should note the low values of parameter *Sa* (as low as 0.4–0.5 µm) after dry and MQL-assisted turning with the diamond insert and after oil mist-assisted turning with the carbide insert. Parameter *Sz* shows high variability. Even though three measurements were carried out and mean values were calculated from them, considerable deviations of this parameter's values occur. Even the theoretical relationship with the rate of feed is not preserved. This is due to 3D measurement since there were single elevations or valleys (especially after machining at the lowest rate of feed) increasing the value of *Sz*. Surface shaping at higher feed rates had a more kinematic-geometrical character. At the feed rate of 0.27 the elevations considerably distant (by the feed rate value) from one another have higher values and there are no longer any other single elevations or valleys between them.

Graphs showing the influence of the cutting parameters and the use of oil mist on the values of box fractal dimension D after turning with respectively the carbide tool and the diamond tool are presented in Figure 2. To better illustrate the changes taking place in the geometrical structure of the surface, reflected in fractal dimension values, selected isometric images of surface roughness are shown in Figures 3 and 4. In Figure 2, one can clearly see that the fractal dimension value decreases as the feed rate increases. This dependence occurs for turning with each of the tools. But the decrease is larger for turning with the polycrystalline diamond insert. No effect of the cutting speed on the box dimension value is noticeable. Another thing clearly visible in the graphs is the lower value of the fractal dimension of the surface obtained by oil mist-assisted turning. This mainly applies to the surface after turning with the uncoated sintered carbide insert. The surface after dry turning is more irregular, with more abrupt and sharp changes in its geometrical structure. Due to the use of oil mist, the wear of the blade is much lower for carbide blades [27]. As a result, the carbide blade stays sharp longer, and less distortion occurs when contouring the surface. Moreover, during turning assisted with cutting fluid, even when the latter is fed in minimal quantities, the intensity of build-up considerably decreases. Undoubtedly the two factors influence the roughness and geometrical structure of the surface, as corroborated by the fractal dimension calculations. Since diamond tools wear out much slower, even during dry turning [27], the effect of oil mist on the surface's geometrical
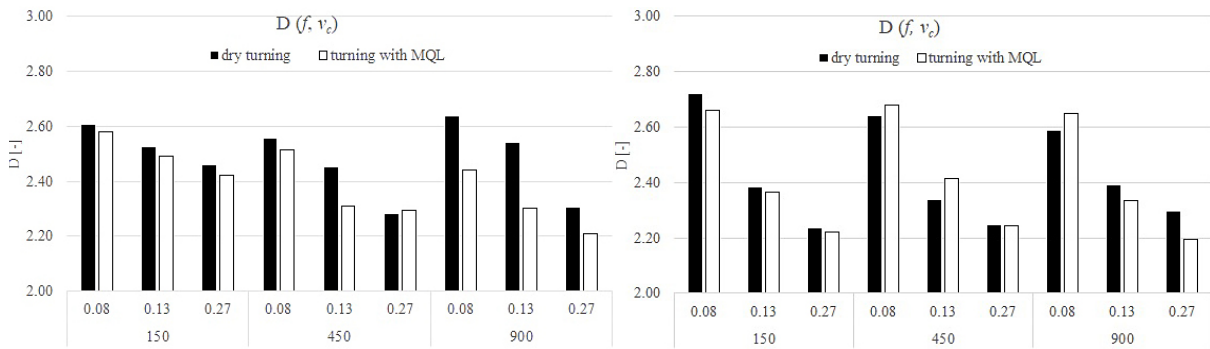
Fig. 2. Influence of turning parameters on box fractal dimension values
for surfaces after turning with carbide tool (left) and diamond tool (right)

structure and the fractal dimension values is not so marked. Moreover, an increase in the box dimension was noticed after turning with MQL.

An interesting effect was obtained after turning at rough machining parameters (v_c = 150 m/min, f = 0.27 mm/rev). There is a distinct difference in the surface fractal dimension between turning with the carbide insert and turning with the diamond insert. In the case of the latter tool, the surface is much less irregular (Fig. 3) and the box dimension assumes much lower values (2.22–2.24 for the diamond insert and 2.42–2.46 for the carbide insert). The geometrical structure of the surface after turning with the

polycrystalline diamond insert shows no other tool marks than the directional ones consistent with the kinematic-geometrical mapping of the cutting edge (particularly the structure after turning with MQL (Fig. 3d)). The surface after dry turning with the uncoated carbide insert shows disturbed directional tool marks and ill-defined valleys (Fig. 3a). The latter include areas resembling flashes or build-up residues. The surface after turning with MQL shows scarce small valleys, which could have been caused by the pulling of the reinforcement out of the surface.

Figure 4 shows surfaces generated at the cutting parameters typical of finishing. After turning
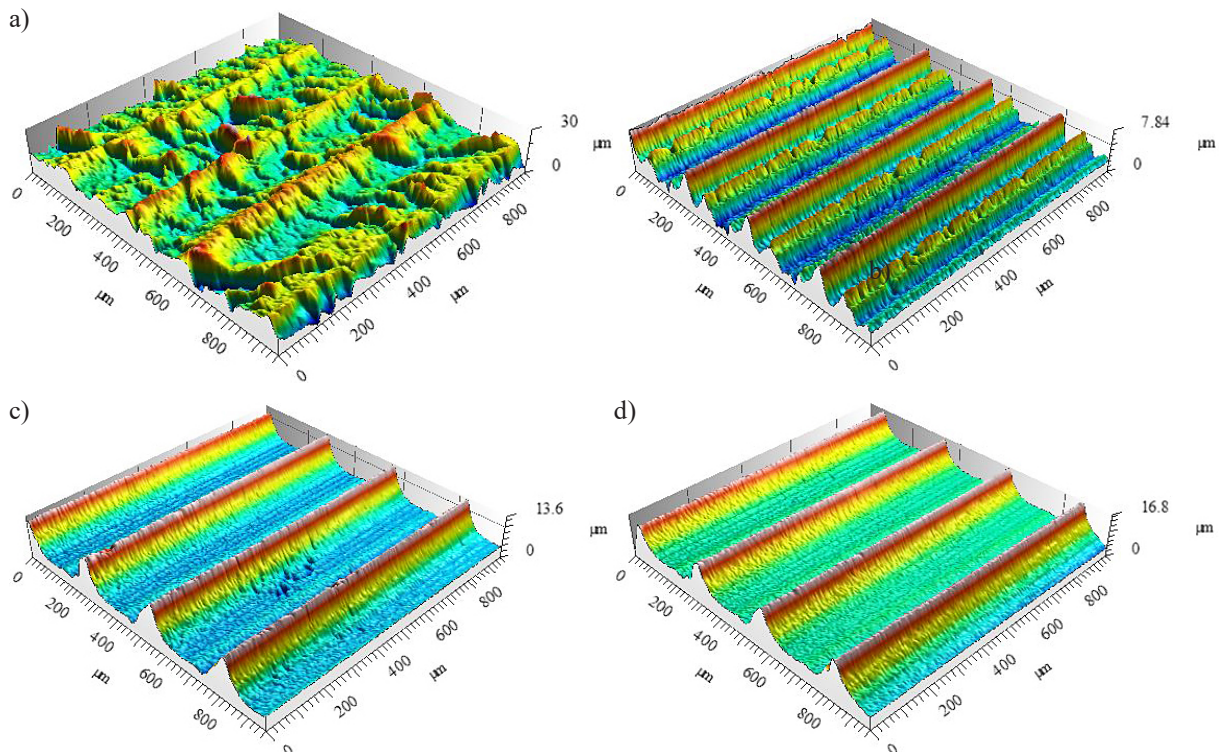
Fig. 3. Surfaces obtained by turning at cutting speed of 150 m/min and feed rate of 0.27 mm/rev: a) tool H10, dry turning; b) tool H10, turning with MQL; c) tool CD10, dry turning; d) tool CD10, turning with MQL
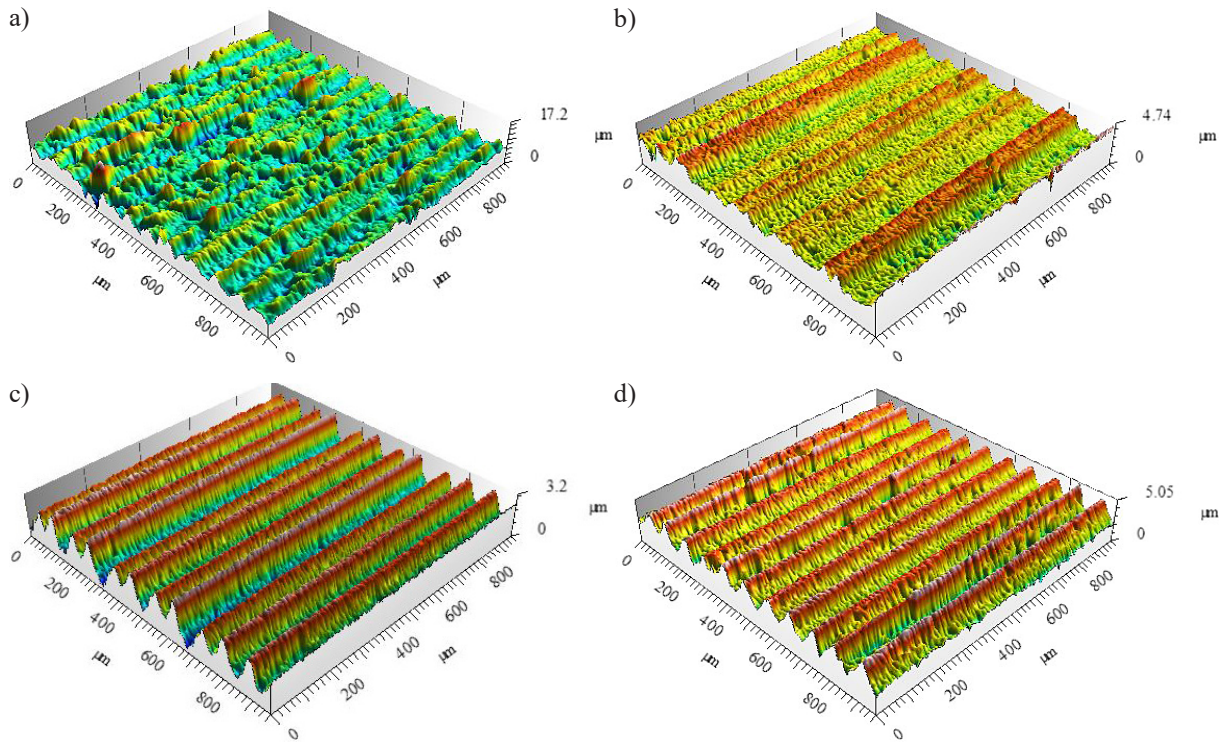
Fig. 4. Surfaces obtained by turning at cutting speed of 900 m/min and feed rate of 0.08 mm/rev: a) tool H10, dry turning; b) tool H10, turning with MQL; c) tool CD10, dry turning; d) tool CD10, turning with MQL

with the carbide tool, no characteristic directional tool marks can be discerned. The surfaces after turning with the diamond tool look quite different. After both dry turning and MQL-assisted turning, one can clearly see elevations and valleys distant from one another by the feed rate value. After oil mist-supported turning, small disturbances and irregularities on the slopes of the elevations are visible. This is reflected in the fractal dimension value (2.59 for dry turning and 2.64 for MQL turning). The effect of oil mist is clearly visible on the surfaces shaped using the uncoated carbide tool. The use of cutting fluid considerably reduced the irregular changes on the surface. After dry turning, numerous irregular and random elevations filled with the material are visible on the surface. The change in the surface's geometrical structure is reflected in the change of the fractal dimension value from 2.64 after dry turning to 2.44 after MQL-assisted turning.

In the next analytical step, the coefficient of the correlation between the fractal dimension and the selected roughness parameters for a constant cutting speed and a constant feed rate was calculated. As it is very rarely found to be correlated with the standard surface parameters, the fractal dimension is generally considered to be an additional parameter describing the geometrical structure of a surface. Since the subject of the investigations was a heterogeneous composite material, this regularity could be disturbed. Tables 4 and 5 show the correlation between the box dimension and parameter *Sa*. Figure 5 shows a plot of the relationship between the fractal dimension *D* and the *Sa* parameter after turning with v_c = 150 m/min. One can clearly see that an inverse correlation between these parameters holds for the surface obtained by dry turning with the carbide blade at the constant cutting speed. As the rate of feed increases, these surfaces become to some degree more regular and the disturbances associated with the lateral flow of the material decline. On the other hand, as the rate of feed increases, so does the value of parameter *Sa*. As, after dry turning, the value of these parameters amounted to 0.8–0.9, this increase is not so large. The correlation after turning with MQL is weaker because due to the use of oil mist, the *Sa* value drops significantly at the lowest feed rates, and the subsequent increase in the *Sa* value with the feed rate is faster than the reduction of unevenness and the fractal dimension.
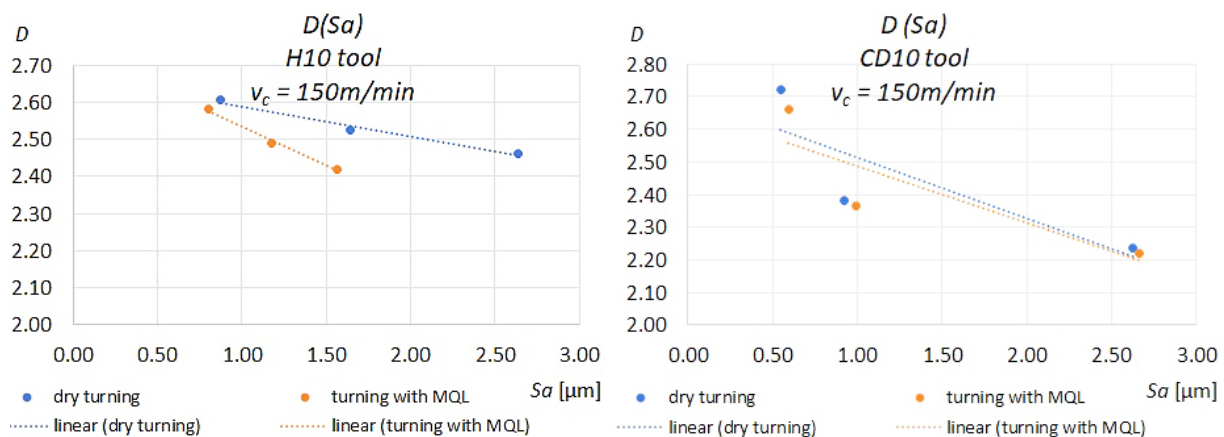
Due to the already mentioned certain deviations in the values of parameter *Sz,* the correlation between this parameter and the fractal dimension is much less strong than in the case of *Sa* (Tables

Table 4. Coefficients of correlation between changes in fractal dimension *D* and roughness parameter *Sa* after machining with tool H10 at constant cutting speeds v_c and constant feed rates *f*

Machining conditions	Cutting speed v_c [m/min]	Correlation coefficient	Feed rate *f* [mm/rev]	Correlation coefficient
dry	150	-0.99	0.08	0.75
MQL		-1.00		0.81
dry	450	-1.00	0.13	0.84
MQL		-0.76		1
dry	900	-0.99	0.27	0.21
MQL		-0.9		1

Table 5. Coefficients of correlation between changes in fractal dimension *D* and roughness parameter *Sa* after machining with tool CD10 at constant cutting speeds v_c and constant feed rates *f*

Machining conditions	Cutting speed v_c [m/min]	Correlation coefficient	Feed rate *f* [mm/rev]	Correlation coefficient
dry	150	-0.84	0.08	-0.26
MQL		-0.86		-0.51
dry	450	-0.72	0.13	0.86
MQL		0.91		0.94
dry	900	-0.85	0.27	0.98
MQL		-0.84		0.98

Fig. 5. Fractal dimension *D* versus parameter *Sa* at constant cutting speed v_c = 150 m/min

6 and 7). Any individual changes on the surface, reflected in the values of parameter *Sz*, are not reflected in the box dimension value calculated as an average for the whole surface. Since the correlation between these parameters is much stronger, in the case of the surface shaped using the diamond insert, one can assume that machining with this tool reduces the risk of occurrence of deep cracks or high elevations and peaks. Thus in the case of the diamond tool, the predictability of the quality of the generated surface and its features is higher. Also, less intensive wear of diamond blades increases the predictability of the service properties for the surface of composites machined with this kind of tool.

Then parameters *Ssk* and *Sku* were analysed and compared with the fractal dimension.

Even though the parameters are classified as height parameters, they are dimensionless and can be regarded as statistical parameters. Since they are characterized by very high sensitivity to single changes in the profile, it is much better to analyse them when taken from measured surfaces. *Ssk* is a coefficient of surface asymmetry, i.e. it defines the skewness of the distribution of elevations. It has an averaging character and can assume positive values in the case of structures with numerous elevations or negative values for surfaces with predominant valleys. The more distant from zero this parameter is, the more heterogenous the material distribution. In the case of composite surfaces after turning, it assumes mostly positive values.

Table 6. Coefficients of correlation between changes in fractal dimension *D* and roughness parameter *Sz* after machining with tool H10 at constant cutting speeds v_c and constant feed rates *f*

Machining conditions	Cutting speed v_c [m/min]	Correlation coefficient	Feed rate *f* [mm/rev]	Correlation coefficient
Dry	150	-0.96	0.08	0.15
MQL		0.61		0.94
Dry	450	0.51	0.13	0.9
MQL		-0.65		1.00
Dry	900	-0.76	0.27	0.94
MQL		-0.97		-0.61

Table 7. Coefficients of correlation between changes in fractal dimension *D* and roughness parameter *Sz* after machining with tool CD10 at constant cutting speeds v_c and constant feed rates *f*

Machining conditions	Cutting speed v_c [m/min]	Correlation coefficient	Feed rate *f* [mm/rev]	Correlation coefficient
Dry	150	-0.88	0.08	0.03
MQL		-0.9		-0.92
Dry	450	-0.33	0.13	0.93
MQL		-0.99		0.91
Dry	900	-0.89	0.27	1.00
MQL		-0.84		-0.36

Its value increases with the rate of feed. The effect of the cutting speed is small – *Ssk* increases slightly with the cutting speed. The use of oil mist and the kind of tool material have no unequivocal influence on the value of this parameter. An analysis of the coefficients of the correlation between *Ssk* and the fractal dimension shows that the correlation is strong, but only at a constant cutting speed (Tables 8 and 9). For the surface obtained after dry turning with the diamond tool, the correlation coefficient for each of the constant cutting speeds assumes the value of -1. No correlation between the parameters calculated at a constant feed rate was noticed. This is undoubtedly due to the lack of any dependence between cutting speed changes and the values of parameter *Ssk*.

Finally, roughness parameter *Sku* and its correlation with the fractal dimension were analysed. This parameter is a measure of the sharpness of the amplitude density curve and so can be referred to as a coefficient of flattening.

Table 8. Coefficients of correlation between changes in fractal dimension *D* and roughness parameter *Ssk* after machining with tool H10 at constant cutting speeds v_c and constant feed rates *f*

Machining conditions	Cutting speed v_c [m/min]	Correlation coefficient	Feed rate *f* [mm/rev]	Correlation coefficient
Dry	150	-1.00	0.08	-0.56
MQL		-0.88		-0.13
Dry	450	-0.9	0.13	-0.98
MQL		-1.00		-0.87
Dry	900	-0.91	0.27	-0.99
MQL		-0.96		-0.87

Table 9. Coefficients of correlation between changes in fractal dimension *D* and roughness parameter *Ssk* after machining with tool CD10 at constant cutting speeds v_c and constant feed rates *f*

Machining conditions	Cutting speed v_c [m/min]	Correlation coefficient	Feed rate *f* [mm/rev]	Correlation coefficient
Dry	150	-1	0.08	0.32
MQL		-0.95		0.74
Dry	450	-1	0.13	0.56
MQL		-0.79		-0.89
Dry	900	-1	0.27	1

Table 10. Coefficients of correlation between changes in fractal dimension *D* and roughness parameter *Sku* after machining with tool H10 at constant cutting speeds v_c and constant feed rates *f*

Machining conditions	Cutting speed v_c [m/min]	Correlation coefficient	Feed rate *f* [mm/rev]	Correlation coefficient
Dry	150	0.94	0.08	-1.00
MQL		0.82		0.25
Dry	450	0.61	0.13	0.93
MQL		0.97		-0.98
Dry	900	0.47	0.27	-1.00
MQL		0.88		-0.97

Table 11. Coefficients of correlation between changes in fractal dimension *D* and roughness parameter *Sku* after machining with tool CD10 at constant cutting speeds v_c and constant feed rates *f*

Machining conditions	Cutting speed v_c [m/min]	Correlation coefficient	Feed rate *f* [mm/rev]	Correlation coefficient
Dry	150	-0.99	0.08	-0.43
MQL		-0.99		-0.9
Dry	450	-0.16	0.13	0.88
MQL		-0.99		0.48
Dry	900	-0.96	0.27	-0.66
MQL		-0.8		-0.79

Generally, surfaces obtained by turning with a carbide tool are characterized by a higher value of *Sku* (as a rule, above 3) than the surfaces after machining with a diamond tool (most often below 3). This is significant as the boundary value for this parameter is 3. When *Sku* is below this limit, the elevations are longer and the peaks are more filled with the material. Whereas, above this boundary, the elevations become shorter and sometimes sharper. This is visible in the surface images presented in Figures 3 and 4. Diamond turned surfaces have more pronounced peaks with more material on them. The surfaces turned with the carbide tool do not show such distinct peaks, but those that are visible have more pointed shape. Moreover, the effect of the feed rate on *Sku* is noticeable. For the surfaces turned with the carbide tool as the rate of feed increases, the value of *Sku* slightly decreases. The reverse can be observed for the surfaces shaped with the diamond tool. The examination of the correlation between *Sku* and the fractal dimension did not show the correlation to be strong in any of the cases (Tables 10 and 11). This indicates that the fractal dimension does not describe features similar to the ones described by *Sku* and does not reflect changes in the character of peaks and their filling with the material. Therefore one can assume that the fractal dimension will not express the bearing strength of the surface of composites.

CONCLUSIONS

This study has shown that it is not only possible, but also advisable to use fractal analysis to describe the surface of composites after turning. The fractal dimension can be treated as an additional, and sometimes alternative, roughness parameter. The following conclusions emerge from the analyses:

- the fractal dimension changes when the cutting parameters, the tool or the way of lubricating the cutting zone are changed. The feed has the greatest influence, the value of the box fractal dimension decreases with the increase of the feed - the highest values were obtained at a feed rate of 0.08 mm/rev, while the lowest at a feed rate of 0.27 mm/rev.
- In the case of composites, similarly to the case of other materials, the fractal dimension describes the degree of surface irregularity. It has values above 2.6 for surfaces where numerous irregular adhering particles, or build-up residues were observed on the machined surface. Its lowest values are when the surface is characterized by distinct elevations and depressions with regular slopes.
- The fractal dimension particularly correlates with roughness parameter *Sa* for the surfaces dry turned with the carbide tool, and with parameter *Ssk* for the surfaces obtained after respectively dry turning and MQL-assisted turning with each of the tools. Correlation coefficients equal to 1 were obtained.

The next step in this research should be to explore the possibility of employing wavelet analysis as a tool supplementing the standard analysis of roughness to describe the surface of composites and also of combining wavelet analysis with the fractal dimension to highlight the surface features overlooked by Gaussian analysis and to treat this not only as a supplement, but also as an alternative to Gaussian analysis.

REFERENCES

1. Healey R., Wang J., Chiu W.K., Chowdhury N.M., Baker A., Wallbrink C. A review on aircraft spectra simplification techniques for composite structures. Composites Part C. 2021;5:100–131. https://doi.org/10.1016/j.jcomc.2021.100131

2. Vijaya Ramnath B., Parswajinan C., Dharmaseelan R., Thileepan K., Nithin Krishna K. A review on aluminium metal matrix composites, Materials Today: Proceedings. 2021;46(9):4341–4343. https://doi.org/10.1016/j.matpr.2021.03.600

3. Ramakrishnan G., Vijaya Ramnath B., Naveen E., Gowtham S., Kumar Arun A., Muthuvel M.S., Akil R. A Review on Aluminium Metal Matrix Composites. Advanced Science, Engineering and Medicine. 2018;10(5):263–267.

4. Das M., Mishra D., Mahapatra T.R. Machinability of Metal Matrix Composites: A Review. Materials Today: Proceedings. 2019;18(7):5373–5381. https://doi.org/10.1016/j.matpr.2019.07.564

5. Bhardwaj Ajay R., Vaidya A.M., Shekhawat S.P. Machining of Aluminium Metal Matrix Composite: A Review. Materials Today: Proceedings. 2020;21(2):1396–1402 https://doi.org/10.1016/j.matpr.2020.01.179

6. Mandelbrot B. Les objets fractals: Forme, hasard et dimension. Flammarion; 1975

7. Zhang X., Zheng G., Cheng X., Li Y., Li L., Liu H. 2D fractal analysis of the cutting force and surface profile in turning of iron-based superalloy. Measurement. 2020;151:107–125. https://doi.org/10.1016/j.measurement.2019.107125

8. Niu Z.K, Jiao L., Chen S.Q., Yan P., Wang X.B. Surface quality evaluation in orthogonal turn-milling based on box-counting method for image fractal dimension estimation. Nanomanufacturing Metrology. 2018;1:125–130. https://doi.org/10.1007/s41871-018-0015-x.

9. Panigrahy C., Seal A., Mahato N.K. Quantitative texture measurement of grayscale images: fractal dimension using an improved differential box counting method. Measurement. 2019;147:106859. https://doi.org/10.1016/j.measurement.2019.106859

10. Nayak S.R., Mishra J., Palai G. A modified approach to estimate fractal dimension of gray scale images. Optik. 2018;161:136–145. https://doi.org/10.1016/j.ijleo.2018.02.024.

11. Nayak S.R., Mishra J., Khandual A., Palai G. Fractal dimension of RGB color images. Optik. 2018;162:196–205. https://doi.org/10.1016/j.ijleo.2018.02.066

12. Jing C.L., Tang W. Ga-doped ZnO thin film surface characterization by wavelet and fractal analysis. Applied Surface Science. 2016;364:843–849. http://dx.doi.org/10.1016/j.apsusc.2015.12.234

13. Jiang C.X., Lu Z.X., Zhou J., Muhammad S.M. Evaluation of fractal dimension of soft terrain surface. Journal of Terramechanics. 2017;70:27–34. https://doi.org/10.1016/j.jterra.2017.01.003.

14. Zuo X., Zhu H., Zhou Y.K., Ding C. Monofractal and multifractal behavior of worn surface in brass-steel tribosystem under mixed lubricated condition. Tribology International. 2016;93:306–317. https://doi.org/10.1016/j.triboint.2015.09.035.

15. Macek W., Marciniak Z., Branco R., Rozumek D., Królczyk G.M. A fractographic study exploring the fracture surface topography of S355J2 steel after pseudo-random bending-torsion fatigue tests. Measurement. 2021:178:109443. https://doi.org/10.1016/j.measurement.2021.109443

16. Macek W. Fractal analysis of the bending-torsion fatigue fracture of aluminium alloy. Engineering Failure Analysis. 2019;99:97–107. https://doi.org/10.1016/j.engfailanal.2019.02.007.

17. Karolczak P., Kowalski M., Wiśniewska M. Analysis of the possibility of using wavelet transform to assess the condition of the surface layer of elements with flat-top structures. Machines. 2020;8(4):1–21. https://doi.org/10.3390/machines8040065

18. Grzesik W., Brol S. Wavelet and fractal approach to surface roughness characterization after finish turning of different workpiece materials. Journal of Materials Processing Technology. 2009;209:2522–2531. https://doi.org/10.1016/j.jmatprotec.2008.06.009

19. Li G.X., Zhang K., Gong J.Z., Jin X. Calculation method for fractal characteristics of machining topography surface based on wavelet transform. Procedia CIRP. 2019;79:500–504.

20. Altintas Y. Manufacturing Automation: Metal Cutting Mechanics, Machine Tool Vibrations, and CNC Design. Cambridge University Press, New York, 2012.

21. Wang H., Chi G., Jia Y., Ge Ch., Yu F., Wang Z., Wang Z. Surface roughness evaluation and morphology reconstruction of electrical discharge machining by frequency spectral analysis. Measurement. 2021;172:108879. https://doi.org/10.1016/j.measurement.2020.108879

22. Karolczak P., Kowalski M., Raszka K.H. The application of fractal analysis to description of brushed steel surfaces. Journal of Machine Engineering. 2020;20(4):99–115. https://doi.org/10.36897/jme/130618

23. Papanikolaou M., Salonitis K. Fractal roughness effects on nanoscale grinding. Applied Surface Science. 2019;467–468:309–319. https://doi.org/10.1016/j.apsusc.2018.10.144

24. Chang Q., Chen D.L., Ru H.Q., Yue X.Y., Yu L., Zhang C.P. Three-dimensional fractal analysis of fracture surfaces in titanium–iron particulate reinforced hydroxyapatite composites: relationship between fracture toughness and fractal dimension. Journal of Materials Science. 2011;46:6118–6123.

25. Kuang X., Zhu Z., Carotenuto A.G., Nicolais L. Fractal Analysis and Simulation of Surface Roughness of Ceramic Particles for Composite Materials. Applied Composite Materials. 1997;4:69–81.

26. Rimpault X., Chatelain J.F., Klemberg-Sapieha J.E., Balazinski M. Tool wear and surface quality assessment of CFRP trimming using fractal analyses of the cutting force signals. CIRP Journal of Manufacturing Science and Technology. 2017;16,:72–80. https://doi.org/10.1016/j.cirpj.2016.06.003

27. Karolczak P., Kołodziej M., Kowalski M. Effectiveness of diamond blades in the turning of aluminium composites. Advances in Science and Technology Research Journal. 2020;14(4);262–272. https://doi.org/10.12913/22998624/127436

28. www.accu-lube.com - Accu-Lube materials